SENSITIVITY OF SPACE-BASED PRECIPITATION MEASUREMENTS

JP7.2 TO CHANGES IN MESOSCALE FEATURES

Joseph Hoch *, Gregory J. Tripoli, Mark Kulie
University of Wisconsin, Madison, Wisconsin

1. INTRODUCTION

The period of January 7th through January 11th, 2005 brought tremendous amounts of rainfall and snowfall throughout the entire state of California. Areas such as Nordhoff Ridge and Opids Camp recorded over 25 inches of equivalent rainfall during the event. The storm caused millions of dollars in damage and at least 10 deaths due to mudslides. This storm was particularly damaging for the region as a similar storm system had just impacted the area from December 26th through January 5th, 2005.

As is the case with many storms in California, the mountainous terrain of the region enhanced the precipitation. Orographically forced precipitation has been the focus of much research attention. Previous studies have commonly focused on the Sierra Nevada region because of the regular occurrence of this type of precipitation enhancement (Marwitz, 1987; Reynolds and Kuciauskas, 1988; Colle and Zeng, 2004; Dettinger et al., 2004; Galewsky and Sobel, 2005).

Orographic precipitation is a challenging quantity to retrieve accurately using space-based passive microwave remote sensing techniques. This is due to the complex interactions between large-scale dynamics and cloud microphysical processes. Inaccurate understanding of microphysics, such as characterizing the properties of precipitation-sized hydrometeors incorrectly, leads to rainfall retrieval error (Mugnai and Smith 1988; Kummerow and Giglio 1994). Platforms such as the Advanced Microwave Scanning Radiometer (AMSR) can be used to retrieve precipitation over the California region.

Recently a new methodology for rainfall retrieval has been considered. Currently, precipitation estimates are made from Cloud Radiation Databases (CRD's) which contain thousands of microphysical profiles that relate brightness temperatures to precipitation intensity. The new retrieval approach will include all the classic information of a CRD but also many large-scale dynamical and thermodynamical tags to further increase the constraints on any given bayesian-based retrieval approach. The Cloud Dynamics and Radiation Database (CDRD) will be formulated using the University of Wisconsin Non-hydrostatic Modeling System (UW-NMS), which is a cloud resolving model (Tripoli, 1992).

In Section 2, the general CDRD concept is discussed. In Section 3, simulation results and sensitivity studies are presented for the January 7th California event. The sensitivity of modeled microwave brightness temperatures to several parameters such as, topography elevation, sea surface temperatures, topography slope, and model resolution are discussed and evaluated for their importance as tags in the CDRD system design. Finally, conclusions are presented in section 4.

2. CDRD CONCEPT

The CDRD system will inherently be a robust system. This system will avoid the use of inversion and will not have to make intangible mathematical or physical approximations to estimate retrieval. Bayesian retrieval methods and forward modeling will be the basis behind precipitation retrieval using the CDRD. At the time of retrieval a satellite overpass in conjunction with dynamic/thermodynamic information, possibly from soundings, ground sensors, or large-scale models (i.e., NAM, GFS, ECMWF), can be used to mine the CDRD for the appropriate microphysical profiles. These profiles will contain the following information at all 34 vertical layers of the UW-NMS simulations.

* *Corresponding author address:* Joseph Hoch, Univ. of Wisconsin, Dept of Atmospheric and Oceanic Sciences, Madison, WI 53715; email: hoch@wisc.edu

Total Condensate Mixing Ratio
Rain Mixing Ratio
Cloud Mixing Ratio
Water Vapor Mixing Ratio
Graupel Mixing Ratio
Aggregate Mixing Ratio
Pristine Crystal Mixing Ratio
Surface Precipitation Rates (Rain, Snow, Aggregate, Pristine Crystal, Graupel)
Surface Skin Temperature
Q1, Q2
Temperature
Pressure
Height
Zonal Wind (U)
Meridional Wind (V)
Vertical Velocity (w)

The final list of dynamical and thermodynamical tags to be paired with these profiles is being compiled. Such tags will include mean sea level pressure, surface pressure, 3-D winds, stability indices, temperature profiles, and many others. Variables such as topography elevation, topography slope, sea surface temperature, and model resolution are all evaluated as potential variables for the CDRD system. If slight changes in any potential tag result in large brightness temperature shifts then these should be included in the CDRD database. The following California case study is used to investigate the sensitivities.

3. CASE STUDY

The UW-NMS is used for simulating the four-day event. A three grid nesting system is used with an outer grid resolution of 50km, middle grid resolution of 10km, and an inner grid resolution of 2km. The largest timestep on the outermost grid is 90 seconds, 22.5 seconds on the middle grid nest, and 11.25 seconds on the innermost grid. The UW-NMS is particularly good at simulating orographically enhanced precipitation due to its unique terrain system, a variable step topography system. Similar mesoscale models represent terrain in various other ways, such as terrain following systems or step topography systems. Terrain following systems have a difficult time resolving very steep topography. Step topography systems have a hard time resolving subtle changes in topography. The UW-NMS terrain system is capable of handling both these cases very well (Tripoli, 1992).

The model used for radiative transfer calculations is the Successive Order of Interaction (SOI) Radiative Transfer Model, developed by Ralf Bennartz and collaborators at the University of Wisconsin. The SOI is a one-dimensional azimuthally averaged, plane-parallel radiative transfer model. This model includes the effects of scattering from all hydrometeors. The SOI ignores atmospheric polarization but not surface polarization (Heiginger, O'Dell, Bennartz, and Greenwald 2005). This is a hybrid model which uses both the doubling method and the Neumann method. The Neumann method involves successive order of scattering to obtain the upwelling radiance.

Figure 1 shows the synoptic setup that lead to the intense rainfall over the California region. This image is courtesy of the California Nevada River Forecast Center. The main branch of the jet stream brought a low-pressure system off the coast of British Columbia. A relatively strong subtropical jet stream provided the necessary moisture over the entire region. The high-pressure system further west in the Pacific Ocean set up a blocking pattern that kept the jet stream in the shown position for several days. Another low-pressure system became stationary off the coast of California helping to further stream subtropical moisture into the region. During the four day period the precipitable water reached values as high as 1.5 inches. As impulses moved onto the California coast, winds flowing counterclockwise intersected the Sierra Nevada mountain chain and caused heavy orographic precipitation enhancement.

The UW-NMS did an excellent job simulating this particular orographic event. Figure 2 shows several synoptic parameters predicted for January 7^{th}, 2005 at 12Z. Contours of mean sea level pressure show the stalled low-pressure system positioned off the northern California coast. There is a large amount of liquid water content along with low 5km pressure contours clearly showing the two low-pressure systems, including the stationary low off the British Columbia coastline. Also shown is the 3-dimensional wind field. This plot shows the structure of the jet stream over the region. Notice that 1-km wind vectors point nearly perpendicular to the Sierra Nevada mountain range. Neiman et al. showed that winds perpendicular to a mountain range at 1km are one of the best predictors of orographic precipitation. (2002).

To verify the accuracy of the simulations stage IV radar/gauge data is used from the National Centers for Environmental Prediction (NCEP). This data is available over the CONUS at 4km resolution. Figure 3 shows the comparison for accumulated precipitation during the four-day period, January 7th – 11th. These plots show that the UW-NMS is very successful in precipitation prediction for this synoptic/mesoscale event.

To get a sense for how much precipitation is being influenced by the topography of the region the same simulation was run with no mountains. Figure 4 shows the difference in UW-NMS predicted precipitation amounts for the no mountain run minus the control run. Values less than -2 inches are overlaid onto a topography map of California, also produced by the UW-NMS. The largest differences in precipitation exist directly over the mountain ranges.

Since the model produces realistic results radiative transfer calculations are run for the same time period using the SOI model. Any particular brightness temperatures can be simulated with the SOI. Figure 4 shows four simulated microwave brightness temperatures fields at 36.5, 89.0, 150.0, and 183.3 GHz frequencies. These plots correspond to January 8th, 2005 at 12Z.

A significant barrier in microwave remote sensing is simulating accurate brightness temperatures over land. For the purposes of this sensitivity experiment a constant land emissivity of 0.9 was used. Land emissivities may range from 0.4 – 0.9 in many cases. Since our focus is mainly on precipitating regions the land emissivity becomes less of a problem since precipitation, if heavy enough, can block out some land effects.

The brightness temperature fields show many interesting features. For example, the 183.3 GHz frequency, which is a water vapor absorption band, seems to show the presence of gravity waves. These waves are positioned correctly with respect to the Sierra Nevada range.

For the purposes of the sensitivity testing, four variables of particular interest are selected: elevation, slope, sea surface temperature, and resolution. New simulations are run for all of the following cases: (a) elevation is increased/ decreased 500 meters throughout the inner domain, (b) topography slope of the Sierra Nevada chain is increased gradually by raising topography by multiples of 30 meters, starting at the bases of the mountain range (increased 30m) and ending at the apex (increased 600m), (c) sea surface temperatures are increased/decreased 5 degrees Kelvin, and (d) resolution of the innermost grid is increased to 1.6 km and decreased to 6.6km.

Figure 6 shows the change in brightness temperatures for each different adjusted simulation. In each case the new simulation brightness temperature fields are subtracted from the control run brightness temperatures. All of the UW-NMS grids are based on a 252 x 252 grid domain. The scatter plots show the difference in brightness temperatures at each point.

As expected, all investigated parameters show the capability to change the brightness temperatures by a significant amount (20K +). For some parameters, such as the increased sea surface temperature experiment, the brightness temperatures fluctuate by over 100K at some points on the grid.

Sensitivity studies with radar reflectivity factor showed similar results with the same four parameters. The changes in radar reflectivity are statistically significant when compared to the control run.

4. CONCLUSIONS

The above simulations show that the four parameters in question, topography elevation, sea surface temperature, topography slope, and model resolution, play an important role in accurately determining brightness temperatures and radar reflectivity factor. Slight changes in any of these parameters change modeled brightness temperatures by a statistically significant amount.

The global CDRD, being developed for improved passive microwave precipitation retrieval, will include several dynamical and thermodynamical tags to further constrain a bayesian based retrieval algorithm. This concept builds on the current CRD approach. This study has shown that the four parameters in question should be included in a database used for precipitation retrieval purposes. A final list of tags is being compiled and the CDRD is expected to be available in the near future.

5. REFERENCES

Colle B. A., Y. Zeng, 2004: Bulk Microphysical Sensitivities within the MM5 for Orographic Precipitation. Part I: The Sierra 1986 Event, *Mon. Wea. Rev.*, **132**, 2780-2801.

Dettinger M., K. Redmond, D. Cayan, 2004: Winter Orographic Precipitation Ratios in the Sierra Nevada – Large-Scale Atmospheric Circulations and Hydrologic Consequences, *J. Hydrometeor*., **5**,1102-1116.

Galewsky J., A. Sobel, 2005: Moist Dynamics and Orographic Precipitation in Northern and Central California during the New Year's Flood of 1997, *Mon. Wea. Rev*., **6**, 1594-1612.

Heiginger A. K., C. O'Dell, R. Bennartz, T. Greenwald, 2005: The Successive Order of Interaction Radiative Transfer Model, Part I: Model Development, *J. Atmos. Sci*., submitted.

Kummerow C., L. Giglio, 1994: A Passive Microwave Technique for Estimating Rainfall and Vertical Structure Information from Space. Part II: Applications to SSM/I Data, *J. Appl. Meteor*., **33**, 19-34.

Marwitz J. D., 1987: Deep Orographic Storms over the Sierra Nevada. Part II: The Precipitation Processes, *J. Atmos. Sci*., **44**, 174-185.

Neiman P. J., F. M. Ralph, A. B. White, D. E. Kingsmill, P.O. G. Persson, 2002: The Statistical Relationship between Upslope Flow and Rainfall in California's Coastal Mountains: Observations during CALJET, *Mon. Wea. Rev*., **130**, 1468-1492.

Reynolds D. W., A. P. Kuciauskas, 1988: Remote and In Situ Observations of Sierra Nevada Winter Mountain Clouds: Relationships between Mesoscale Structure, Precipitation and Liquid Water, *J. Appl. Meteor*., **27**, 140-156.

Smith E. A., A. Mugnai, 1988: Radiative Transfer to Space through a Precipitation Cloud at Multiple Microwave Frequencies. Part II: Results and Analysis, *J. Appl. Meteor*., **27**, 1074-1091.

Tripoli G. J., 1992: A Nonhydrostatic Mesoscale Model Designed to Simulate Scale Interaction, *Mon. Wea. Rev*., **120**, 1342-1359.

ACKNOWLEDGMENTS

The authors would like to thank Ralf Bennartz and Chris O'Dell with their help on the SOI radiative transfer model.

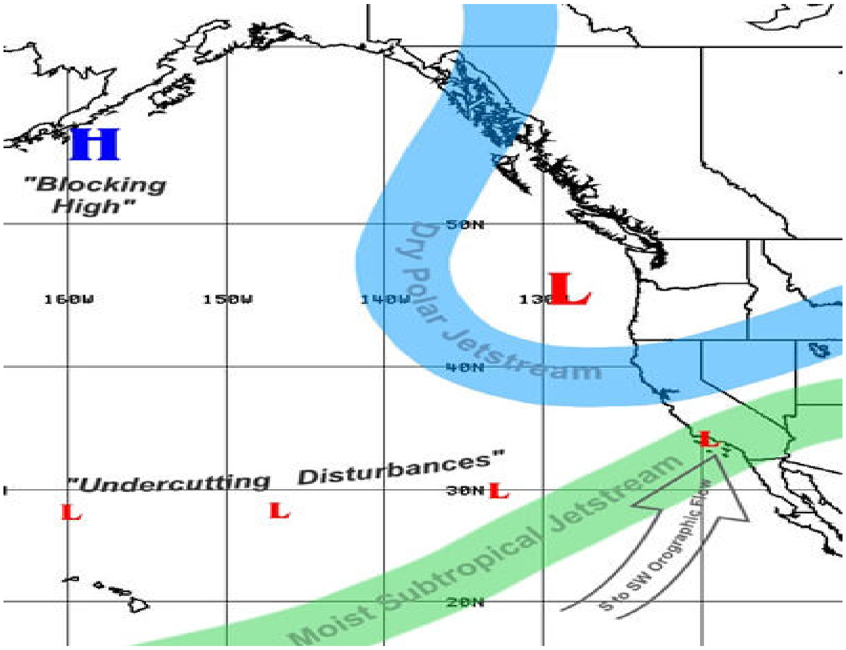

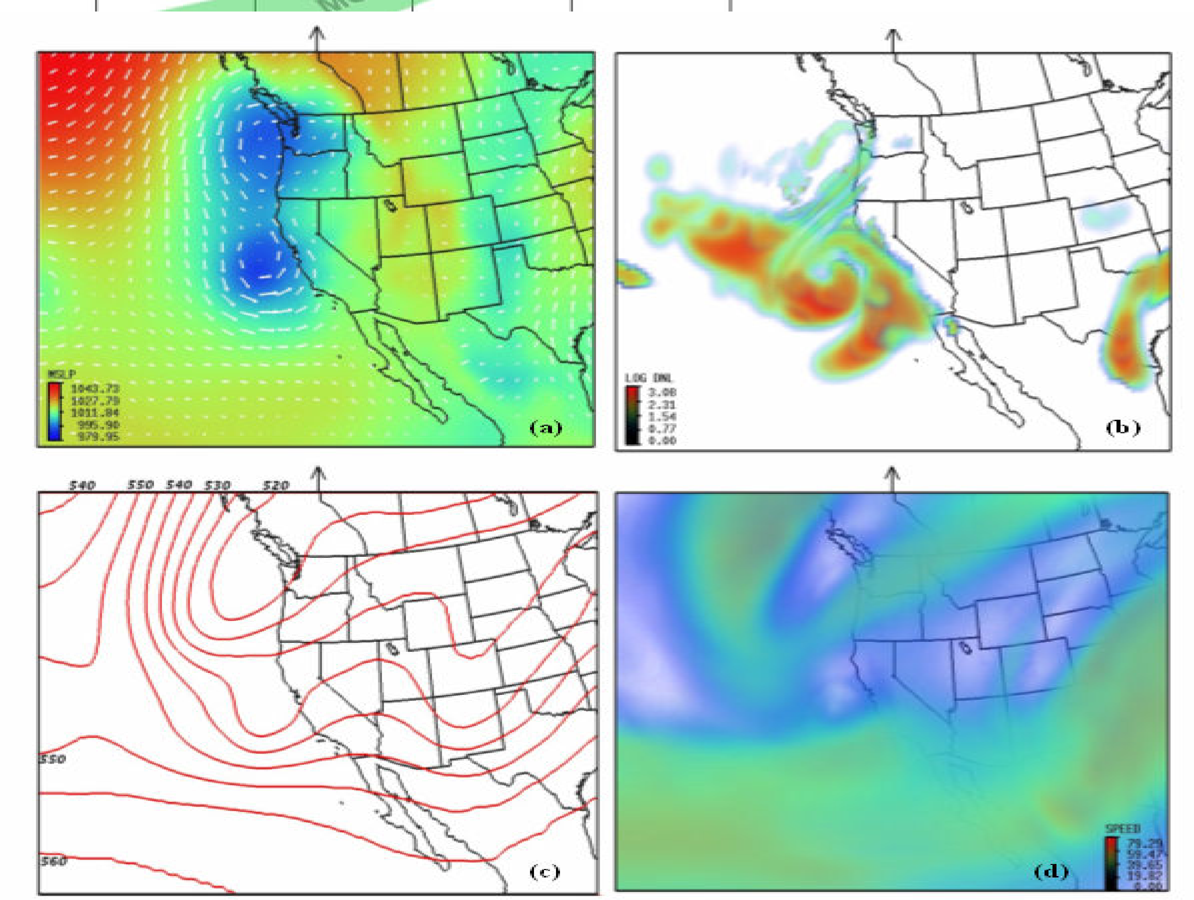

Figure 1. (Left)
Synoptic Setup
January 07 – 12th, 2005

Figure 2. (Below)
(a) Mean Sea Level Pressure and 1km Winds, (b) Log of Liquid Water Content,
(c) 5 km Pressure Contours,
(d) 3-D Wind Field
Valid – January 7th, 2005 12Z

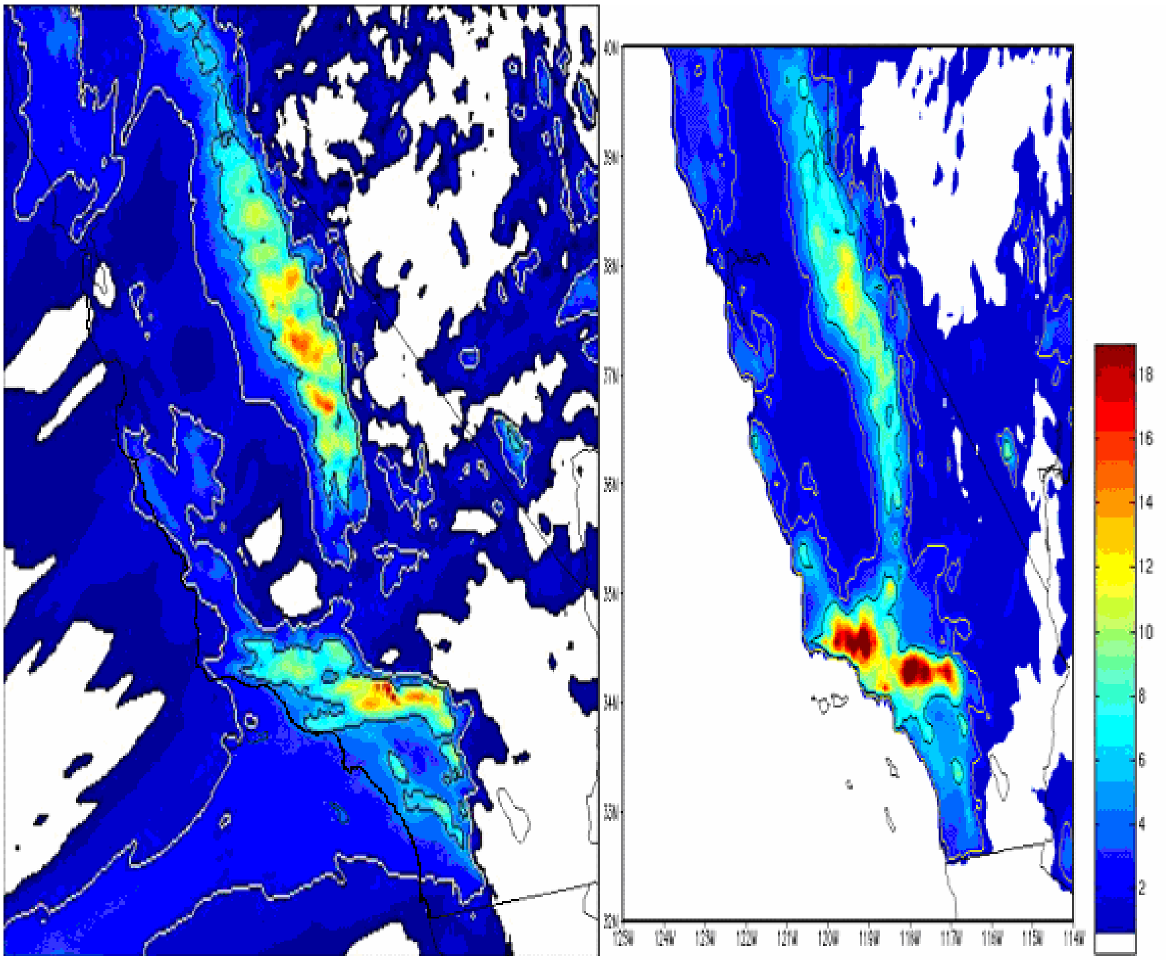

Figure 3. Left: 4 Day Accumulated Rainfall (in) (12Z Jan 07 – 12Z Jan 10) from UW-NMS
Right: 4 Day Accumulated Rainfall (in) (12Z Jan 07 – 12Z Jan 10) from NCEP Stage 4 Radar Data
Yellow Contour – 3 inches
Black Contour – 7 inches

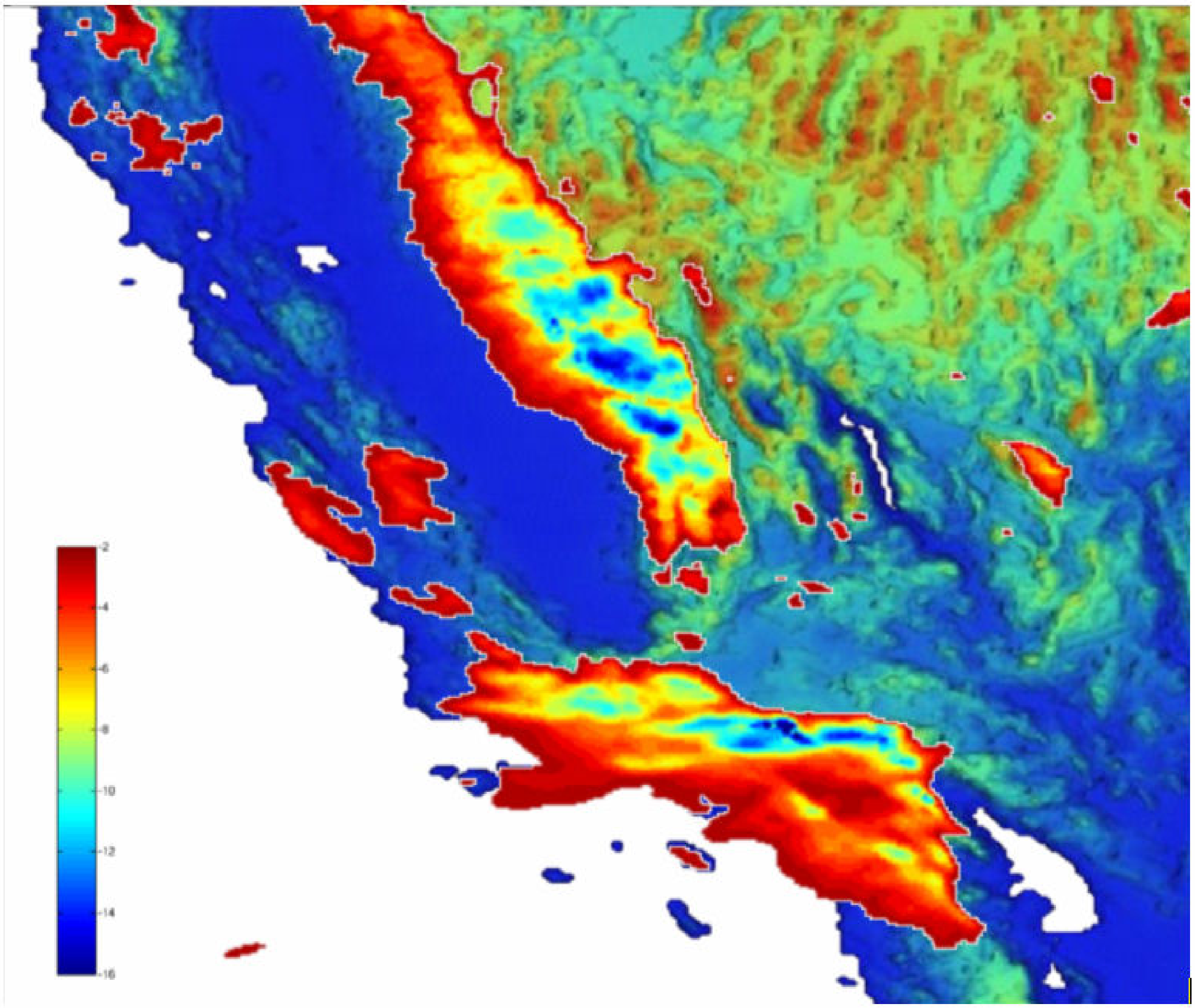

Figure 4. No Mountains Accumulated Precipitation (in) minus
Control Run Accumulated Precipitation (in)

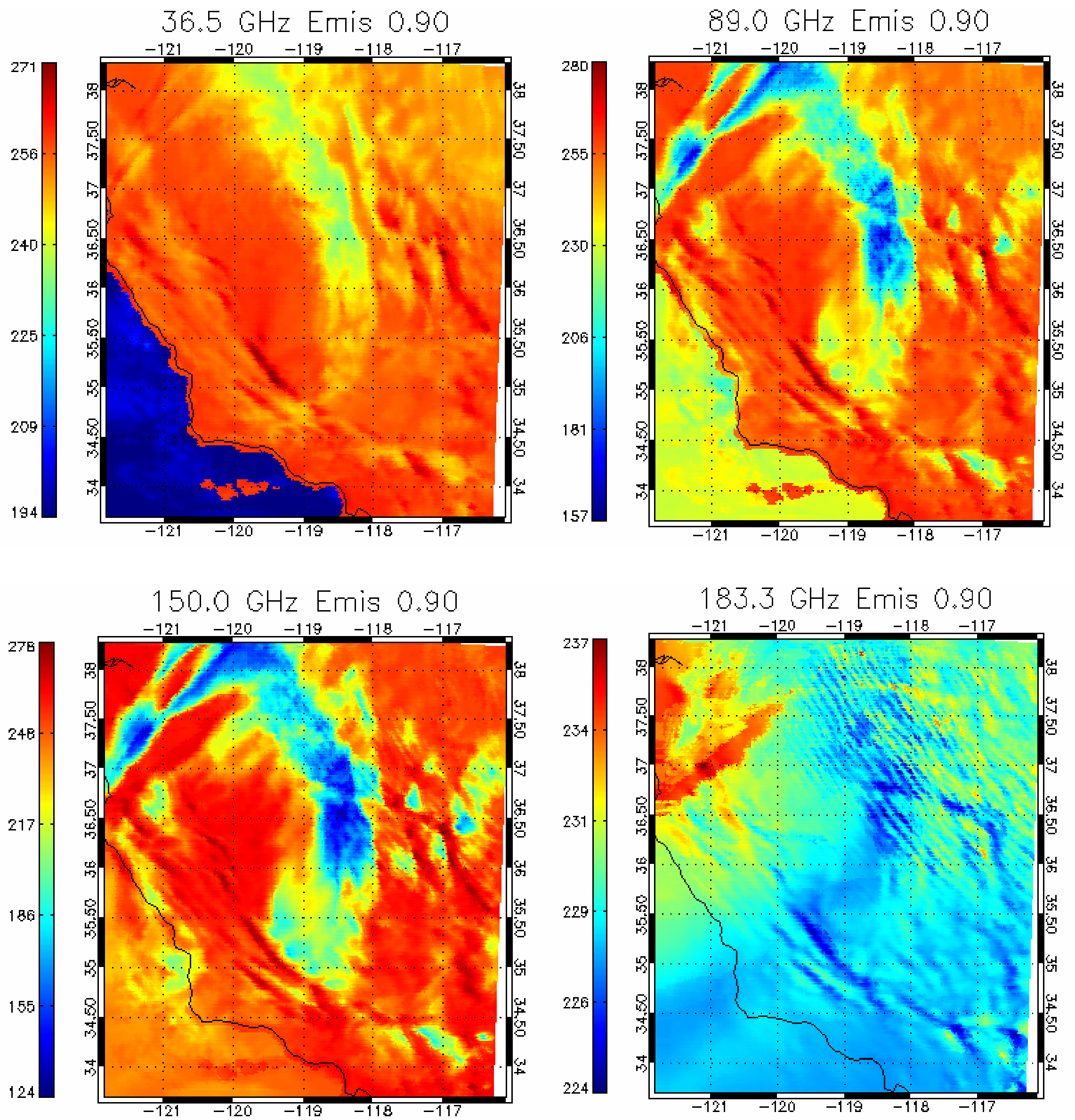

Figure 5. Selected brightness temperatures (K) for 12Z January 8th, 2005

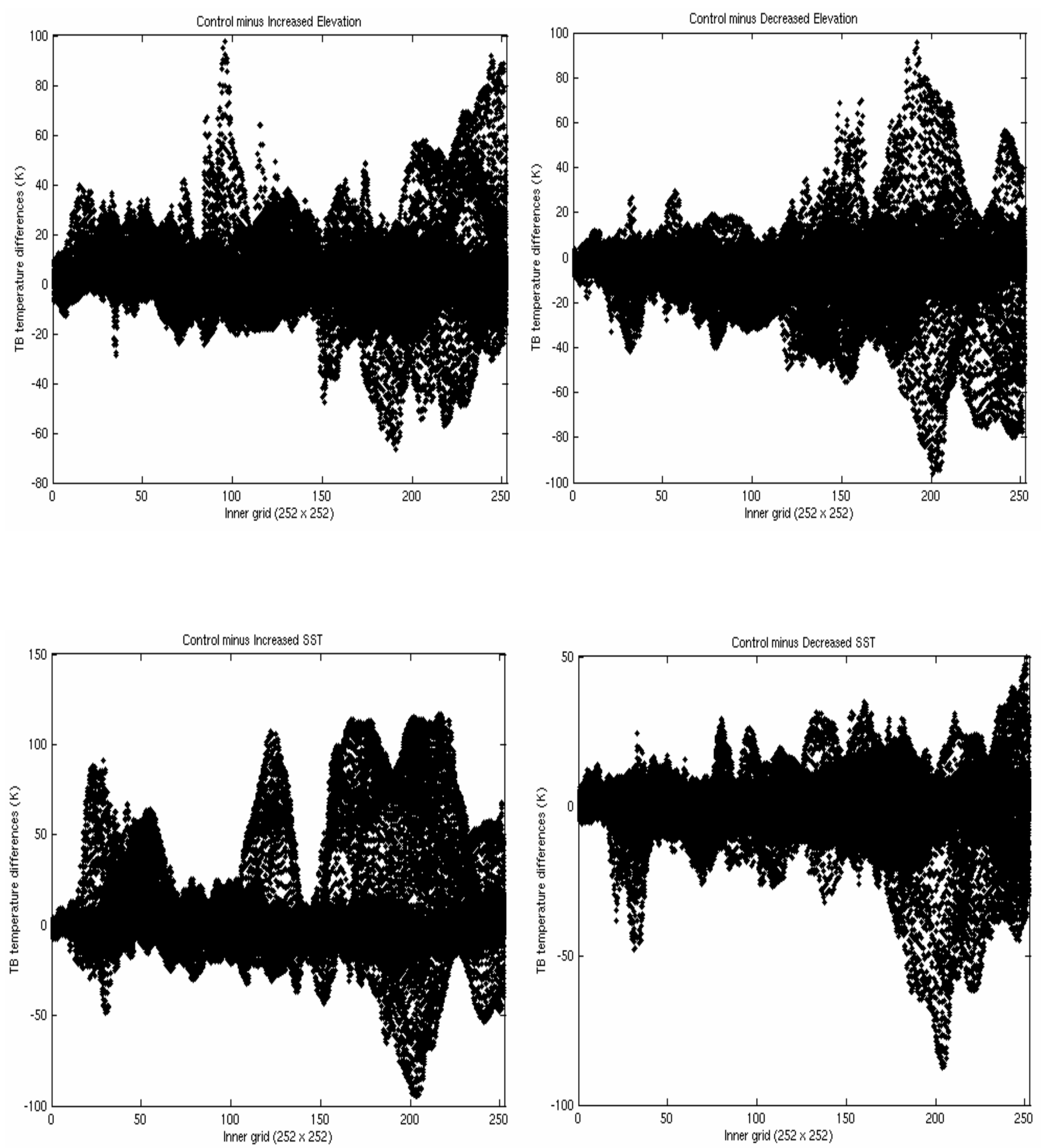

Control minus Increased Elevation
TB temperature differences (K)
Inner grid (252 x 252)
Control minus Decreased Elevation
TB temperature differences (K)
Inner grid (252 x 252)
Control minus Increased SST
TB temperature differences (K)
Inner grid (252 x 252)
Control minus Decreased SST
TB temperature differences (K)
Inner grid (252 x 252)

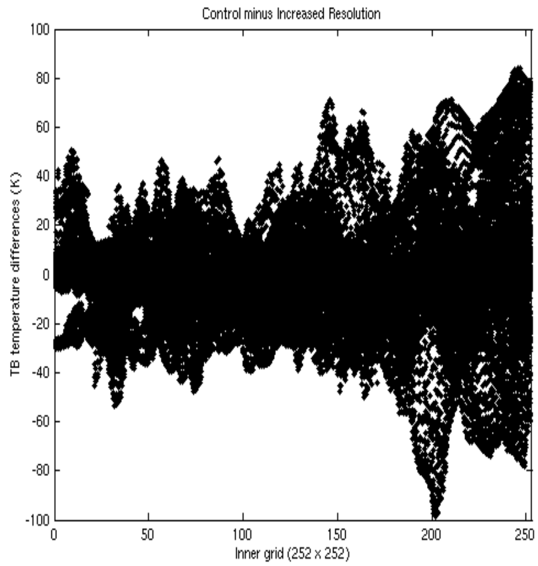

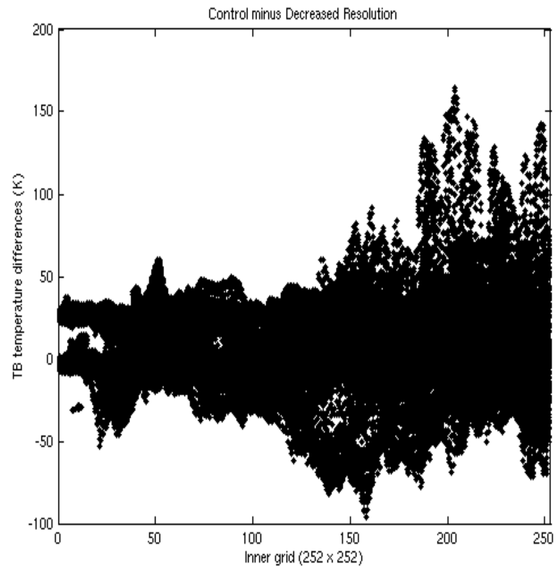

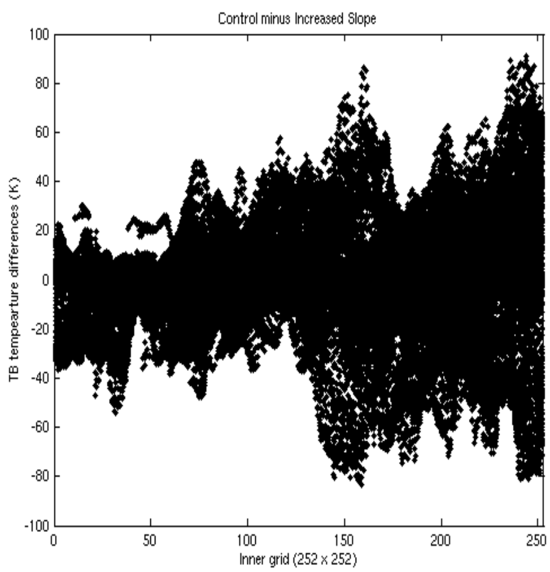

Figure 6. Differences in brightness temperatures for 89 GHz using different sensitivity tests